N.L. thanks the Centre National de la Recherche Scientifique (France) for permission to carry out part of this work at The Pennsylvania State University.

Supplementary Material Available: A variable-temperature NMR study for **5b** (Figure A) and tables of atomic positional parameters, anisotropic thermal parameters, bond lengths, and bond angles for **2**, **5c**, **13'**, **14**, and **20** (31 pages); tables of observed and calculated structure factors (67 pages). Ordering information is given on any current masthead page.

Contribution of Physical Blocking and Electronic Effect to Establishment of Strong Metal-Support Interaction in Rh/TiO_2 Catalysts

Juan P. Belzunegui, Jesus Sanz, and Jose M. Rojo*

Contribution from the Instituto Ciencia de Materiales, CSIC, C/Serrano 115 dpdo, 28006 Madrid, Spain. *Received September 23, 1991. Revised Manuscript Received February 27, 1992*

Abstract: Establishment of strong metal-support interaction in Rh/TiO_2 catalysts has been studied by ^1H NMR spectroscopy as a function of conditions of reduction in H_2: temperature (373-773 K), time, and type of reduction (static or dynamic). Two consecutive stages have been identified: one when the catalyst is reduced below 673 K and the other when the temperature is above 673 K. In the first stage, elimination of hydrogen incorporated into the metal-support interface, by outgassing at 773 K, recuperates hydrogen adsorption on the metal. In the second stage, the outgassing treatment does not recover metal adsorption capacity. Physical blocking of metal adsorption sites by TiO_x species and electronic perturbation of the metal are responsible for the irreversible loss of hydrogen adsorption. From analysis of the NMR line assigned to hydrogen adsorbed on the metal, the relative contribution of both effects to adsorption suppression has been estimated.

Introduction

When catalysts consisting of group VIII metals supported on TiO_2 are reduced in H_2 at high temperatures (about 770 K), the metal capacity to adsorb H_2 and CO is suppressed. This metal behavior, ascribed initially to a strong metal-support interaction (SMSI),[1,2] was explained in terms of bonding between titanium cations and metal atoms, as deduced from theoretical calculations[3] and XPS, XANES, and EXAFS data.[4-11] The other source for the SMSI state consists in geometric blocking of metal adsorption sites[12-20] due to (i) migration of TiO_x ($1 < x < 2$) suboxide species onto the metal or (ii) burial of the metal into the support. In particular, it has been shown[21] by HRTEM that reduction of Rh/TiO_2 catalyst at 773 K produces an amorphization of the TiO_2 surface and a migration of TiO_x overlayers onto metal particles. However, some controversy still exists about the effect of TiO_x species on adsorption suppression. Thus, some authors[22,23] have found that the decrease in CO adsorption is proportional to the amount of metal surface covered by those species, while others[24] have observed a decrease higher than that expected for only geometric blocking. The two considered explanations, electronic and physical blocking, are not mutually exclusive for the SMSI state, and formation of chemical bondings between the metal and TiO_x species has been proposed[7,25,26] as the driving force for migration of those species onto metal particles.

In previous works[27,28] we have shown that incorporation of hydrogen into the metal-support interface decreases hydrogen adsorption on rhodium particles. When hydrogen is removed by outgassing the sample at 773 K, metal particles recover their initial adsorption capacity. Therefore, it seems that different processes such as hydrogen incorporation into the support, migration of TiO_x species onto the metal, and formation of rhodium-titanium bondings are involved during establishment of the SMSI state. The aim of this work is to analyze the experimental conditions in which they are operating and to evaluate their contribution to the metal chemisorption suppression. In this way, reduction in H_2 of an Rh/TiO_2 sample as a function of (i) temperature, (ii) time, and (iii) type of reduction (static and dynamic) has been

(1) Tauster, S. J.; Fung, S. C.; Garten, L. R. *J. Am. Chem. Soc.* **1978**, *100*, 170-175.
(2) Tauster, S. J.; Fung, S. C.; Baker, R. T. K.; Horsley, J. A. *Science* **1981**, *211*, 1121-1125.
(3) Horsley, J. A. *J. Am. Chem. Soc.* **1979**, *101*, 2870-2874.
(4) Greenlief, C. M.; White, J. M.; Ko, C. S.; Gorte, R. J. *J. Phys. Chem.* **1985**, *89*, 5025-5028.
(5) Andêra, V. *Appl. Surf. Sci.* **1991**, *51*, 1-8.
(6) Beard, B. C.; Ross, P. N. *J. Phys. Chem.* **1986**, *90*, 6811-6817.
(7) Sakellson, S.; McMillan, M.; Haller, G. L. *J. Phys. Chem.* **1986**, *90*, 1733-1736.
(8) Koningsberger, D. C.; Martens, J. H. A.; Prins, R.; Short, D. R.; Sayers, D. E. *J. Phys. Chem.* **1986**, *90*, 3047-3050.
(9) Martens, J. H. A.; Prins, R.; Zandbergen, H.; Koninsberger, D. C. *J. Phys. Chem.* **1988**, *92*, 1903-1916.
(10) Sankar, G.; Vasudeban, S.; Rao, C. N. R. *J. Phys. Chem.* **1988**, *92*, 1878-1882.
(11) Resasco, D. E.; Weber, R. S.; Sakellson, S.; McMillan, M.; Haller, G. L. *J. Phys. Chem.* **1988**, *92*, 189-192.
(12) Santos, J.; Phillips, J.; Dumesic, J. A. *J. Catal.* **1983**, *81*, 147-167.
(13) Sadeghi, H. R.; Henrich, V. E. *J. Catal.* **1984**, *87*, 279-282.
(14) Huizinga, T.; Van't Blik, H. F. J.; Vis, J. C.; Prins, R. *Surf. Sci.* **1983**, *135*, 580-596.
(15) Belton, D. N.; Sun, Y.-M.; White, J. M. *J. Am. Chem. Soc.* **1984**, *106*, 3059-3060.
(16) Resasco, D. E.; Haller, G. L. *J. Catal.* **1983**, *82*, 279-288.
(17) Sun, Y.-M.; Belton, D. N.; White, J. M. *J. Phys. Chem.* **1986**, *90*, 5178-5182.
(18) Yokoyama, T.; Asakura, K.; Iwasawa, Y.; Kuroda, H. *J. Phys. Chem.* **1989**, *93*, 8323-8327.
(19) Sanchez, M. G.; Gazquez, J. L. *J. Catal.* **1987**, *104*, 120-135.
(20) Ajayan, P. M.; Marks, L. D. *Nature* **1989**, *338*, 139-141.
(21) Logan, A. D.; Braunschweig, E. J.; Datye, A. K.; Smith, D. J. *Langmuir* **1988**, *4*, 827-830.
(22) Ko, C. S.; Gorte, R. J. *Surf. Sci.* **1985**, *161*, 597-607.
(23) Roberts, S.; Gorte, R. J. *J. Catal.* **1990**, *124*, 553-556.
(24) Levin, M.; Salmeron, M.; Bell, A. T.; Somorjai, G. A. *Surf. Sci.* **1986**, *169*, 123-137.
(25) Belton, D. N.; Sun, Y.-M.; White, J. M. *J. Phys. Chem.* **1984**, *88*, 5172-5176.
(26) Tauster, S. J. *Acc. Chem. Res.* **1987**, *20*, 389-394.
(27) Sanz, J.; Rojo, J. M.; Malet, P.; Munuera, G.; Blasco, M. T.; Conesa, J. C.; Soria, J. *J. Phys. Chem.* **1985**, *89*, 5427-5433.
(28) Belzunegui, J. P.; Sanz, J.; Rojo, J. M. *J. Am. Chem. Soc.* **1990**, *112*, 4066-4068.

0002-7863/92/1514-6749$03.00/0

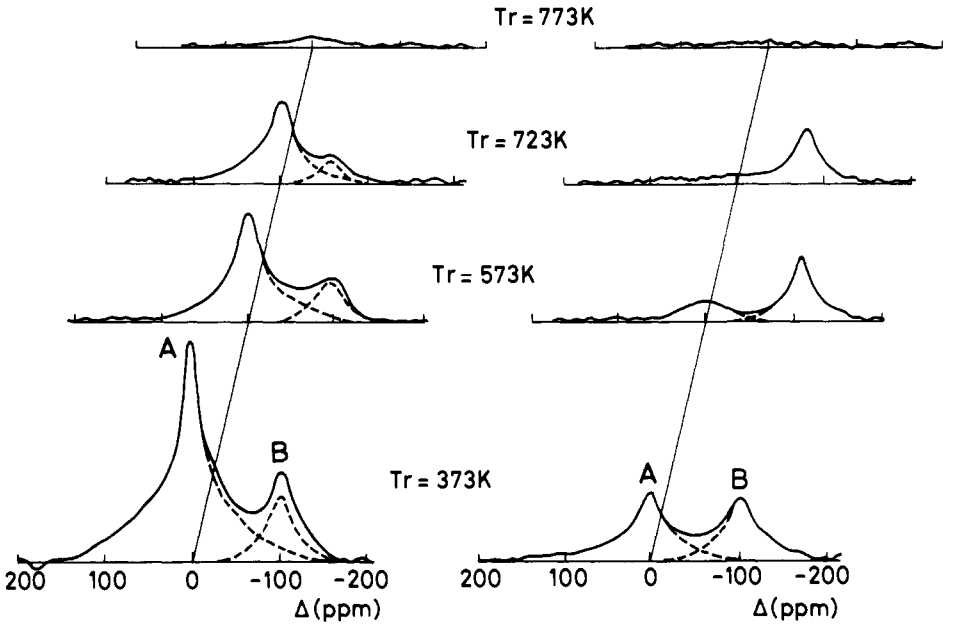

Figure 1. ^1H NMR spectra of the Rh/TiO_2 sample reduced under H_2, under dynamic conditions, at the indicated temperatures and outgassed at 423 K (left) or 773 K (right). After these treatments, the sample was exposed to H_2 (35 Torr) at room temperature before NMR spectra were recorded.

studied. The technique used is ^1H NMR spectroscopy, which allows differentiation of hydrogen adsorbed on the metal from that incorporated into the support.[29] In addition, changes in the hydrogen–metal interaction detected by this technique have been used to follow modifications in electronic properties of the metal during reduction treatments.[28]

Experimental Section

The support used was TiO_2 (Degussa P–25, mostly anatase, BET area = 50 m^2/g). The catalyst was prepared by incipient wetness impregnation of TiO_2 with rhodium trichloride aqueous solution to give 2.5% Rh by weight. The resulting precursor, after being dried in air at 385 K, was reduced under flowing H_2 in two steps (473 K, 2 h; 773 K, 2 h) and subsequently stored in air. TEM (transmission electron microscopy) revealed metal particles with sizes in the range 2–10 nm. Metal dispersion (H/Rh ratio) obtained by volumetric measurements (0.14) is close to that deduced from the NMR spectra (0.12),[29] showing that within experimental error ^1H NMR spectra can be used to evaluate hydrogen adsorption.

Thermal treatments up to 773 K were carried out by placing the sample in Pyrex tubular cells provided with high-vacuum stopcocks. These cells allow the flow of gases through the catalyst as well as outgassing of the sample. Reduction treatments at different temperatures and times were performed in conditions called here either "static" (closed cell with H_2 pressure of 150 Torr) or "dynamic" (H_2 flowing through the catalyst at ca. atmospheric pressure). Oxidation of the sample at 473 or 673 K was always carried out under dynamic conditions.

The Rh/TiO_2 catalyst was first subjected to the standard treatment of reduction in flowing H_2 at 773 K (1 h) and oxidation in flowing O_2 at 673 K (1 h). The experiments carried out in this paper are of two different types: (i) static or dynamic reduction in H_2 at different temperatures and times, followed by outgassing of the sample at 423 or 773 K, in order to study establishment of the SMSI state, and (ii) oxidation in flowing O_2 at 473 (1 h) or 673 K (1 h) after reduction treatments to eliminate partly or completely the SMSI effect.[30] In all cases, the oxidized Rh/TiO_2 sample was heated in flowing H_2 at 373 K (1 h) and outgassed at 423 K to clean metal particles.

NMR spectra were recorded at room temperature with a SXP 4/100 Bruker spectrometer. The frequency used was 75 MHz and the number of accumulations was chosen to get a signal–to–noise ratio higher than 20. Intensity determination of NMR lines was made by comparison of their integrated intensity with that of an external mica specimen.

Results

^1H NMR spectra of an Rh/TiO_2 sample reduced in flowing H_2 at increasing temperatures and exposed to H_2 (35 Torr) at room temperature are shown in Figure 1. Two lines are observed: line A centered at the resonance frequency and assigned to proton species located on the support and line B shifted upfield due to adsorbed hydrogen on rhodium particles.[29] Hydrogen adsorption on the sample deduced from an increment in intensity of NMR spectra agrees with that obtained by volumetric measurements.[31] Taking into account that intensity and chemical shift of line B depend on H_2 pressure[29] and reduction extent of the support,[27,28] the NMR spectra were always recorded on the sample exposed to the same H_2 pressure (35 Torr). This pressure was chosen because of (i) the relative high amount of hydrogen adsorbed on metal particles and (ii) the high sensitivity of chemical shift to reduction treatments. In this figure, when the sample is reduced at increasing temperatures and outgassed at 423 K (left) before H_2 adsorption at 295 K, a decrease in the intensity of lines A and B as well as in the chemical shift of line B is observed. When the sample reduced at the indicated temperatures is outgassed at 773 K (right), the intensity of line A decreases again while the intensity and the chemical shift of line B increase as compared with those corresponding to the sample outgassed at 423 K. In

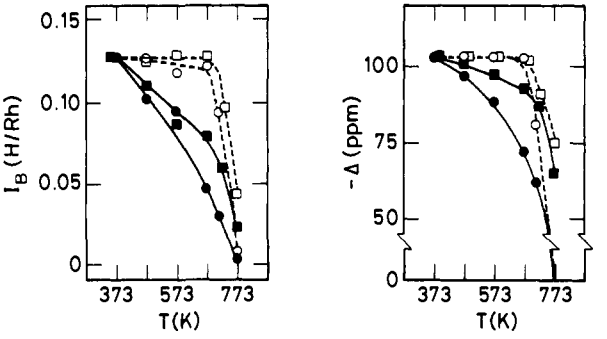

Figure 2. Variation of intensity (I_B) and chemical shift (Δ) of line B vs reduction temperature. The Rh/TiO_2 sample was reduced in an accumulative process at increasing temperatures in static (■) or dynamic conditions (●) and outgassed at 423 K after each treatment. Reductions were carried out for 1 h in dynamic and 2 h in static conditions at each temperature. Open squares and circles correspond to the sample outgassed at 773 K after reduction in static and dynamic conditions, respectively. In all cases, represented values of I_B and Δ were measured at $p(H_2)$ = 35 Torr and room temperature.

(29) Sanz, J.; Rojo, J. M. *J. Phys. Chem.* **1985**, *89*, 4974–4979.
(30) Belzunegui, J. P.; Rojo, J. M.; Sanz, J. *J. Phys. Chem.* **1991**, *95*, 3463–3465.
(31) Belzunegui, J. P. Ph.D. Thesis, Universidad Complutense, Madrid, 1992.

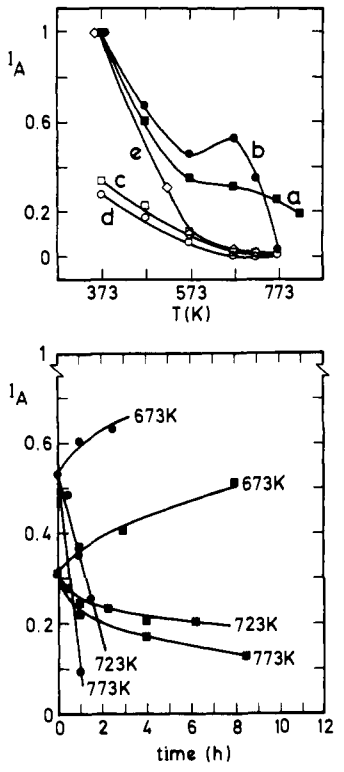

Figure 3. Top: Variation of intensity (I_A) of nonshifted line A against reduction temperature. The Rh/TiO_2 sample was reduced in an accumulative process at increasing temperature in static (■) or dynamic (●) conditions and outgassed at 423 K after each reduction treatment. Reductions were carried out for 1 h in dynamic and 2 h in static conditions at each temperature. Open squares and circles correspond to the sample outgassed at 773 K after static or dynamic reductions, respectively. For comparison, the intensity variation of ^1H NMR spectra of the TiO_2 sample used as support, subjected to dynamic reduction at increasing temperatures and outgassed at 423 K, is also represented (◇). Intensity values were normalized with respect to those obtained for Rh/TiO_2 and TiO_2 samples reduced at 373 K and outgassed at 423 K. Bottom: Effect of reduction time on intensity (I_A) of line A for different temperatures. The Rh/TiO_2 sample was previously reduced in static or dynamic conditions at increasing temperatures up to 673 K and then reduced again at 673, 723, or 773 K for increasing times in static (■) or dynamic (●) conditions. After each reduction treatment the sample was outgassed at 423 K.

the case of the sample reduced at 773 K and outgassed at 423 K, line B disappears from the NMR spectrum (SMSI state) and outgassing of the sample at 773 K does not recover it.

Variation of intensity (I_B) and chemical shift (Δ) of line B vs reduction temperature for static and dynamic conditions is shown in Figure 2. It is observed that I_B decreases with reduction temperature in the range 373–773 K, showing the progressive establishment of the SMSI state. Moreover, the decrease of Δ in this range of temperature indicates a modification in the hydrogen–rhodium interaction, which has been associated with reduction of the support.[27,28] The variation of both parameters is more significant for dynamic than static reductions. When the sample is outgassed at 773 K (dashed curves), after static or dynamic reductions in the range 373–673 K, I_B and Δ increase to their initial values, corresponding to the sample reduced at 373 K. However, for reduction temperatures above 673 K, the same outgassing treatment only produces a partial recuperation in I_B and Δ values. In the case of dynamic reduction at 773 K, the subsequent outgassing of the sample at 773 K does not affect appreciably the values of both parameters. Therefore, two stages related to different phenomena are detected in the adsorption suppression of rhodium particles: one in the range of reduction temperatures 373–673 K and the other between 673 and 773 K.

Intensity variation of the nonshifted line (I_A) vs reduction temperature is shown in Figure 3. For static and dynamic reductions I_A decreases between 373 and 573 K (curves a and b),

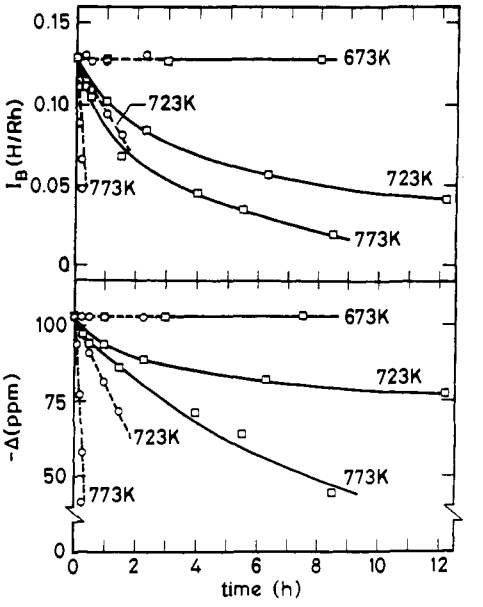

Figure 4. Effect of reduction time on intensity (I_B) and chemical shift (Δ) of line B for different temperatures. The Rh/TiO_2 sample was first reduced in an accumulative process up to 673 K and then reduced at 673, 723, or 773 K for increasing times in static (□) or dynamic (○) conditions. After reduction treatments at 673, 723, or 773 K the sample was outgassed at 773 K and exposed to H_2 (35 Torr) at room temperature. Initial values of I_B and Δ (for $t = 0$) coincide with those obtained at 673 K (dashed curves of Figure 2).

which is due to the surface dehydroxylation of the support, as observed for the TiO_2 sample alone (curve e). Between 573 and 673 K, I_A increases in dynamic reductions and a plateau is observed for static conditions. Above 673 K, a decrease of I_A is again detected in both cases. After each reduction treatment, outgassing of the sample at 773 K produces a significant decrease of I_A (curves c and d). The effect of reduction time on I_A is also shown in this figure. The Rh/TiO_2 sample was previously reduced in an accumulative process up to 673 K and then reduced at 673, 723, or 773 K for different times in static or dynamic conditions, i.e. initial values of I_A (for $t = 0$) coincide with those corresponding to static and dynamic reductions at 673 K in the top portion of Figure 3. The kinetics at 673 K show that I_A increases and its variation is similar for static and dynamic reductions. On the contrary, when the sample is reduced at 723 or 773 K, I_A diminishes with time, the decrease being faster when reduction is done at higher temperatures and under dynamic conditions. Therefore, no qualitative differences are found between both types of reduction, and the maximum of I_A vs T observed for dynamic reduction (curve b) must be related to a more important incorporation of hydrogen below 673 K and a faster elimination of it above this temperature. In static reductions, the incorporation and elimination of hydrogen species is slower, thus explaining the observed plateau (curve a). The opposite trends of I_A vs time below and above 673 K coincide with the two stages identified in the analysis of I_B and Δ (Figure 2).

In order to study in the second stage the irreversible loss of hyrogen adsorption on the metal against the outgassing treatment, we have examined I_B and Δ as a function of reduction time for different temperatures (Figure 4). The Rh/TiO_2 sample was subjected to an accumulative reduction treatment up to 673 K and reduced again at 673, 723, and 773 K for increasing times. After these treatments, the sample was outgassed at 773 K to eliminate the reversible contribution and exposed to H_2 (35 Torr) at room temperature. It is observed that I_B and Δ do not change appreciably with time for reduction at 673 K, but these parameters decrease for increasing times when reduction is carried out at 723 or 773 K. In the last two cases, at a given reduction time, I_B and Δ are lower for higher temperatures, and at the same time and temperature, the value of both parameters is lower for dynamic than for static reductions.

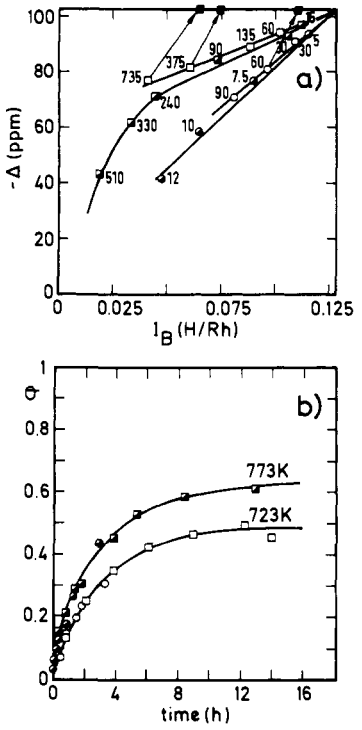

Figure 5. (a) Plot of chemical shift (Δ) vs intensity (I_B) of line B. Values of Δ and I_B are taken from Figure 4. The numbers indicate the time (min) used in static (squares) or dynamic (circles) reductions at 723 K (□, ○) and 773 K (■, ●). Solid squares correspond to the sample oxidized at 473 K after a particular reduction treatment, and they are linked with those corresponding to the reduced sample by an arrow. In all cases, Δ and I_B values were measured at $p(H_2)$ = 35 Torr. The metal surface covered by TiO_x species (θ) has been estimated by subtraction of the intensity of line B of the sample oxidized at 673 K (I_{B0} = 0.128 H/Rh) from that of the sample oxidized at 437 K after each reduction treatment (solid squares). These values were normalized with respect to I_{B0}. (b) Plot of θ vs time used in static (squares) or dynamic (circles) reductions at 723 K (□, ○) and 773 K (■, ●).

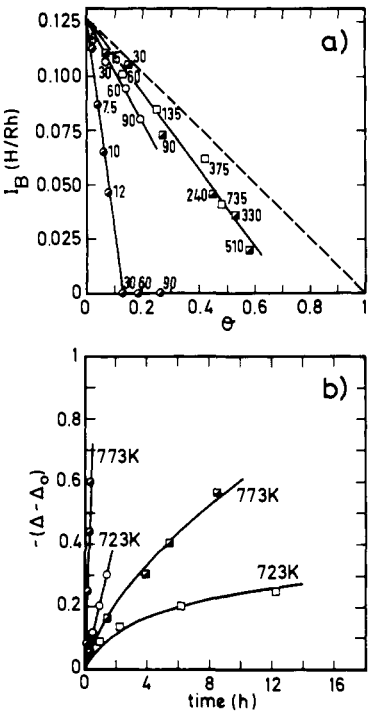

Figure 6. (a) Plot of intensity (I_B) of line B vs metal surface covered by TiO_x species (θ). I_B and θ values correspond to the sample reduced in static (squares) or dynamic (circles) conditions at 723 (□, ○) and 773 K (■, ●) for the indicated times (min). (b) Plot of the electronic perturbation of the metal (Δ − Δ_0) vs time used in reduction treatments at 723 and 773 K. Squares and circles correspond to static and dynamic reductions, respectively. The electronic perturbation was deduced from subtraction of the chemical shift of line B ($p(H_2)$ = 35 Torr) of the sample subjected to a reduction treatment (Δ) from that of the sample oxidized at 473 K (Δ_0) after the reduction treatment. These values were normalized with respect to Δ_0 (−103 ppm).

Discussion

Two stages during establishment of the SMSI state have been identified from ^1H NMR data (Figures 2 and 3). In the first stage (373–673 K), incorporation of hydrogen into the support produces a decrease of hydrogen adsorption on the metal, which is higher when reduction was carried out under dynamic conditions. Thus, at 673 K the adsorption loss is ca. 40 and 60% for static and dynamic reductions, respectively. Outgassing of the sample at 773 K after reduction treatments recovers the metal adsorption capacity. From ESR and NMR results, the incorporated hydrogen has been assigned[27] to hydride-like species placed in oxygen vacancies at the metal–support interface. In the second stage (above 673 K), the outgassing treatment only produces a partial recuperation of I_B and Δ parameters, and the irreversible loss of hydrogen adsorption must be related to other phenomena. In this stage, a decrease of I_A for static and dynamic reductions is also observed. The decrease, more significant for longer times and higher temperatures, indicates that incorporated hydrogen into the support in the first stage is now eliminated.

In order to correlate the irreversible adsorption loss with electronic perturbation of the metal, variation of Δ vs I_B for the sample reduced above 673 K is shown in Figure 5a. The sample reduced in static or dynamic conditions at 723 and 773 K for different times was outgassed at 773 K and then exposed to H_2 (35 Torr) at room temperature. In this figure, Δ and I_B decrease with reduction time in agreement with what is observed in Figure 4. However, different dependences between Δ and I_B are found, and the slope of observed variations is higher when reductions were carried out in dynamic reductions and at higher temperatures. Therefore, a given Δ value is associated with different I_B values depending on reduction treatments. When the electronic perturbation is eliminated by oxidation of the sample at 473 K, different I_B values are also obtained (see the solid squares in the horizontal line of Figure 5a). The oxidation treatment recovers the starting chemical shift value (Δ_0 = −103 ppm), but the maximum hydrogen adsorption is not attained because TiO_x species remain on the metal blocking adsorption sites.[30] Those species are only removed from the metal by oxidation of the sample at 673 K (point I_{B0} = 0.128 H/Rh and Δ_0 = −103 ppm in this figure). Therefore, the difference between line B intensity of the sample oxidized at 673 K (I_{B0}) and that of the sample oxidized at 473 K (I_{B473}) after each reduction treatment can be used[30] to estimate the hydrogen adsorption loss due to the extent of metal surface covered by TiO_x species (θ).

The influence of temperature, time, and type of reduction on adsorption suppression due to physical blocking of metal adsorption sites is shown in Figure 5b. The blocked surface (θ) increases with (i) reduction time (rapidly for short times and slowly for times higher than 4 h) and (ii) reduction temperature. However, θ is not appreciably affected by the type of reduction (static or dynamic). The value θ = 1, corresponding to the total adsorption inhibition, seems difficult to attain although an amorphous TiO_x overlayer on rhodium particles has been observed by TEM.[21] This fact has been explained on the basis that TiO_x overlayers are partly porous for hydrogen thus allowing its adsorption on the metal.[21,30]

A representation of hydrogen adsorption (I_B) vs metal surface covered by TiO_x species (θ) is shown in Figure 6a. It is observed that I_B decreases for increasing θ. If I_B were only affected by the extent of covered metal surface, intensity values should decrease in a linear manner following the dashed line represented in this figure. As the decrease of I_B is more significant than that expected for only physical blocking, it is necessary to admit other causes in order to explain the low I_B values. Similar results were obtained in the case of CO adsorption on Rh foil covered by TiO_x species where the presence of an electronic effect has been proposed.[24] In our Rh/TiO_2 sample, an electronic perturbation of the metal

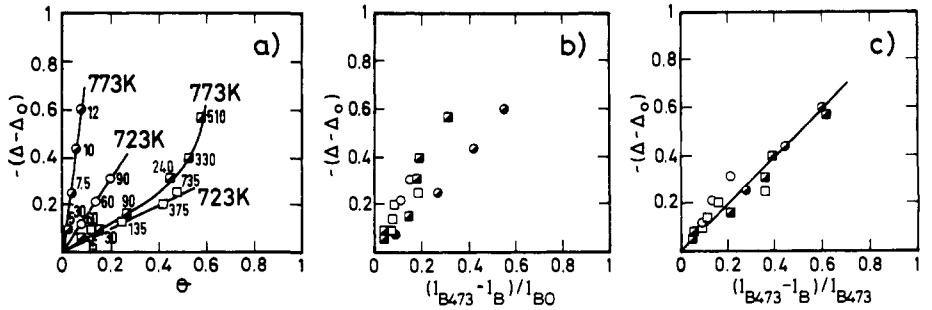

Figure 7. Plots of electronic perturbation of the metal ($\Delta - \Delta_0$) as a function of adsorption suppression due to (a) physical blocking by TiO_x species (θ) and (b and c) electronic effect ($I_{B473} - I_B$). In (b) and (c) adsorption suppression was normalized to hydrogen adsorption on the sample oxidized at 673 K (I_{BO}) and 473 K (I_{B473}), respectively. I_{BO} is the maximum adsorbed hydrogen on the metal while I_{B473} represents hydrogen adsorption on the metal surface not covered by TiO_x species. Squares and circles correspond to reductions in static and dynamic conditions respectively at 723 and 773 K for the indicated times (min). In all cases, chemical shift and intensity of line B were measured at $p(H_2)$ = 35 Torr.

is involved according to variation of the Δ parameter, and its contribution to adsorption suppression should be more significant when the sample is reduced under dynamic conditions and at higher temperatures.

Taking into account that changes in chemical shift of line B during reduction treatments are mostly associated with a modification in electronic properties of the metal,[27,28] the difference between the chemical shift of line B of the sample subjected to a certain reduction treatment (Δ) and that of the sample oxidized at 473 K after each reduction treatment ($\Delta_0 = -103$ ppm) has been used to estimate the electronic perturbation of the metal. It is observed that ($\Delta - \Delta_0$) increases with reduction time (Figure 6b) and the variation is more important (i) for higher reduction temperatures and (ii) when reductions were carried out under dynamic conditions. Low ($\Delta - \Delta_0$) values correspond to I_B values close to the dashed line (Figure 6a), while I_B values far from the dashed line are associated with high ($\Delta - \Delta_0$) values. Therefore, modification in electronic properties of the metal seems to be related to adsorption suppression besides that due to physical blocking.

In order to ascertain whether electronic perturbation of the metal is associated with TiO_x species covering metal particles, ($\Delta - \Delta_0$) as a function of θ is represented in Figure 7a. In all cases, electronic perturbation of the metal increases with the rising extent of covered metal surface for each reduction treatment. However, the increase of ($\Delta - \Delta_0$) is more significant at higher temperatures and for dynamic reductions. As an example, dynamic reduction at 773 K for 12 min and static reduction at the same temperature for 15 min produce the same covered metal surface (ca. 8%), but electronic perturbation of the metal is much higher when reduction is carried out under dynamic conditions. It is clear that although electronic perturbation increases with the extent of covered metal surface for each reduction treatment, it depends mainly on another factor, which is affected by temperature and reduction type (static or dynamic).

On the other hand, the electronic perturbation of the metal has been analyzed as a function of adsorption suppression once the contribution of physical blocking has been excluded (Figure 7b). The adsorption suppression has been obtained from subtraction of line B intensity, measured on the sample oxidized at 473 K after each reduction treatment (I_{B473}), from that obtained on the reduced sample (I_B). These values have been normalized with respect to the maximum adsorption capacity (I_{BO} = 0.128 H/Rh). In this figure, it is observed that ($\Delta - \Delta_0$) increases with the $(I_{B473} - I_B)/I_{BO}$ ratio, but there is some dispersion in the data. However, if the adsorption suppression is referred to the metal surface not covered by TiO_x species, i.e. to line B intensity of the sample oxidized at 473 K after each reduction treatment (I_{B473}), a good linear dependence between both parameters is obtained (Figure 7c). From these results, it is deduced that electronic perturbation of the metal accounts for a part of the detected adsorption suppression. The fact that electronic perturbation and physical blocking are operating in the loss of hydrogen adsorption on the metal explains why Δ and I_B parameters are not correlated by a unique relationship in Figure 5a.

Table I. Relative Contribution of Physical Blocking and Electronic Effect to Adsorption Suppression in the Rh/TiO_2 Sample Subjected to Static and Dynamic Reductions at 723 and 773 K for Different Times and Outgassed at 773 K after Reduction Treatments[a]

reduction treatments			relative loss of hydrogen adsorption (%)	
type	temp, K	time, min	physical blocking	electronic effect
static	723	60	13	7
		135	25	8
		375	42	9
		735	48	19
static	773	15	8	4
		30	15	6
		90	27	15
		240	45	19
		330	53	18
		510	58	26
dynamic	723	30	8	8
		60	14	11
		90	20	17
dynamic	773	5	3	8
		7.5	5	27
		10	6	42
		12	8	55
		30	13	87

[a] The values were deduced from line B intensity of the ^1H NMR spectra of the sample exposed to H_2(35 Torr) at room temperature.

On the basis that metal adsorption loss is due to the sum of both effects, their relative contribution has been evaluated (Table I). In general, adsorption suppression associated with physical blocking and electronic effect increases with time and temperature, but the contribution of metal electronic perturbation is favored in dynamic reductions. Thus, for the sample reduced at 773 K this effect is much higher than that of physical blocking. On the contrary, when the sample is reduced in static conditions, adsorption suppression due to physical blocking increases faster than that associated with electronic perturbation of the metal, and the first contribution is higher than the second one. As deduced from analysis of Figure 3, static and dynamic reductions of the Rh/TiO_2 sample above 673 K produce a dehydroxylation and elimination of incorporated hydrogen. These processes lead to oxygen vacancies near metal particles and rhodium–titanium bonding could be formed.[7-9,11] In this way, the higher contribution of electronic effect detected for dynamic reductions suggests a higher number of rhodium–titanium bonds. These bonds would be mainly established between TiO_x species and metal particles; however, we cannot exclude their formation at the metal–support interface.

Conclusions

Hydrogen adsorption on metal particles decreases progressively when Rh/TiO_2 catalyst is reduced in H_2 at increasing temperatures in the range 373–773 K. Although this is a continuous process

two consecutive stages have been identified. In the first stage (373–673 K), the decrease of hydrogen adsorption is accompanied by an incorporation of hydrogen into the support.[27] After the hydrogen is removed by outgassing of the sample at 773 K, metal particles recover their initial electronic properties and adsorption capacity.[28] In the second stage (above 673 K), the incorporated hydrogen is eliminated and two new factors responsible for adsorption suppression are operating: (i) physical blocking by TiO_x species of metal adsorption sites and (ii) electronic perturbation of the metal, due to formation of rhodium–titanium bonds between metal particles and TiO_x species and/or reduced support.[7-9,11] The effect of both phenomena increases with temperature and time of reduction, but their relative contribution depends on reduction conditions. Adsorption suppression due to electronic perturbation of the metal is enhanced in dynamic reductions while physical blocking is not appreciably affected by the type of reduction. In static conditions the small electronic contribution makes physical blocking the preferentially detected effect. The electronic perturbation is eliminated by oxidation of the sample at 473 K, but removal of TiO_x species from the metal requires that oxidation be carried out at 673 K.[30] In this case electronic properties and adsorption capacity of the metal are completely recovered.

Acknowledgment. This research was supported by Grants MAT 88-0223 and MAT 91-1080 from the Comision Interministerial de Ciencia y Tecnologia (CICYT). J.P.B. thanks the Ministerio de Educación y Ciencia of Spain for a postgraduate fellowship. We thank C. Alonso, I. Sobrados, and T. G. Somolinos for helpful technical assistance.

Registry No. Rh, 7440-16-6; TiO_2, 13463-67-7; H_2, 1333-74-0.

Adsorption and Decomposition of Acetylene on Si(100)-(2×1)

P. A. Taylor,[†] R. M. Wallace,[‡] C. C. Cheng,[†] W. H. Weinberg,[§] M. J. Dresser,[∥] W. J. Choyke,[⊥] and J. T. Yates, Jr.*[,†]

Contribution from the Surface Science Center, Department of Chemistry, University of Pittsburgh, Pittsburgh, Pennsylvania 15260. *Received December 16, 1991*

Abstract: The adsorption and decomposition of acetylene on Si(100)-(2×1) have been studied in ultrahigh vacuum by Auger electron spectroscopy, temperature-programmed desorption, and changes in the partial pressure of acetylene as measured by a quadrupole mass spectrometer during the formation of a monolayer. Acetylene was found to chemisorb onto Si(100)-(2×1) via a mobile precursor. The difference between the activation energy for desorption from the precursor and that for reaction from the precursor into the chemisorbed state was found to be $(E_d - E_r) = 1.9 \pm 0.6$ kcal mol^{-1}. At a low surface temperature, reaction from the precursor state dominates, giving a chemisorption probability of unity at submonolayer coverages. The saturated acetylene coverage is measured to be one C_2H_2 per Si_2 dimer. Thermochemical arguments are presented, which indicate that acetylene bonds as a di-σ species to dimer sites in which the Si–Si dimer bond has been cleaved. Chemisorbed acetylene was found to undergo two thermal reactions. A minor pathway (<5%) involves acetylene desorption, and a major pathway (>95%) involves the dissociation of acetylene to produce chemisorbed carbon and H_2 (g). At temperatures above 800 K, the surface carbon begins to diffuse into the bulk of the silicon crystal.

I. Introduction

The interaction of hydrocarbons with silicon surfaces forms the basis for various technological processes for the production of silicon carbide films.[1-5] The processes of chemical vapor deposition[1-3] and plasma deposition[4,5] of silicon carbide films involve elementary chemical reactions which have not been elucidated in detail, even for simple hydrocarbon reactants.

While chemical vapor deposition (CVD) involves the interaction of gas-phase reactants with surfaces which are heated, it is important to study adsorption at low surface temperatures in order to separate reactions of low activation energy (such as surface migration and adsorption) from reactions of higher activation energy (such as C–H and C–C bond scission in the chemisorbed species). All of these reactions are involved in CVD processes at high temperatures.

At low temperatures, silicon interacts differently with the C–C σ-bonds of saturated hydrocarbons and the C–C π-bonds of unsaturated hydrocarbons.[6] Saturated hydrocarbons do not chemisorb on Si(100) at low temperatures. Unsaturated molecules such as ethylene and propylene chemisorb with high probability and with strong bonding on Si(100).[7,8] In this paper we extend the study of unsaturated hydrocarbon chemistry on Si(100) to acetylene.

Acetylene, like propylene and ethylene, adsorbs with high probability on Si(100) at 105 K; upon heating, approximately 95% of the chemisorbed acetylene thermally dissociates on the surface. This is accompanied by the desorption of hydrogen and the retention of carbon adatoms which diffuse into the bulk silicon above approximately 800 K. The diffusion of carbon adatoms into the silicon lattice forms a layer which will be referred to as "Si–C", which may be viewed as a precursor to the CVD growth of silicon carbide. The remaining 5% of acetylene desorbs without decomposition with an activation energy indicative of strong chemical bonding of chemisorbed acetylene.

[†] Department of Chemistry, University of Pittsburgh.
[‡] Present address: Texas Instruments, Inc., Central Research Laboratories, MS147, Dallas, TX 75265.
[§] Present address: Department of Chemical Engineering, University of California, Santa Barbara, CA 93106.
[∥] Present address: Department of Physics, Washington State University, Pullman, WA 99163.
[⊥] Present address: Department of Physics, University of Pittsburgh, Pittsburgh, PA 15260.

(1) Nishino, S.; Powell, J. A.; Will, H. A. *Appl. Phys. Lett.* **1983**, *42*, 460.
(2) Addamiano, A.; Sprague, J. A. *Appl. Phys. Lett.* **1984**, *44*, 525.
(3) Bozso, F.; Yates, J. T., Jr.; Choyke, W. J.; Muehlhoff, L. *J. Appl. Phys.* **1985**, *57*, 2771.
(4) Catherine, Y.; Turban, G.; Grolleau, B. *Thin Solid Films*, **1981**, *76*, 23.
(5) Mahan, A. H.; von Roedern, B.; Williamson, D. L.; Madan, A. *J. Appl. Phys.* **1985**, *57*, 2717.
(6) Bozack, M. J.; Taylor, P. A.; Choyke, W. J.; Yates, J. T., Jr. *Surf. Sci.* **1986**, *177*, L933.
(7) Clemen, L. L.; Wallace, R. M.; Taylor, P. T.; Dresser, M. J.; Weinberg, W. H.; Choyke, W. J.; Yates, J. T., Jr. *Surf. Sci.* **1992**, *268*, 205.
(8) Bozack, M. J.; Choyke, W. J.; Muehlhoff, L.; Yates, J. T., Jr. *Surf. Sci.* **1986**, *176*, 547.

0002-7863/92/1514-6754$03.00/0